Applications of optical tweezers and an integrated force measurement module for biomedical research

Jin-Wu Tsai[1], Bing-Yao Liao[2], Chun-Cheng Huang[3], Wen-Liang Hwang[2], Da-Wei Wang[2], Arthur E. Chiou[3], and Chi-Hung Lin[1]*

[1]Institute of Microbiology and Immunology, National Yang-Ming University, Taipei, Taiwan, ROC
[2]Institute of Information Science, Academia Sinica, Nankang, Taipei, Taiwan, ROC
[3]Institute of Electrical Engineering, National Dong Hwa University, Shoufeng, Hualien, Taiwan, ROC

ABSTRACT

Optical tweezers are useful for manipulating biological samples and measuring biological forces. In the present study, we have integrated a forward scatter analysis (FORSA) module into the "single-beam gradient force optical tweezers". The entire set-up was then incorporated onto an inverted microscope. In the FORSA module, a Helium-Neon probing laser was spotted (at a slightly out-of-focus way) onto the object being trapped by the infrared laser-based tweezers and generated a diffraction pattern. Images of the diffraction pattern were captured by a charge-coupled device (CCD), and digitized and processed by a computer. We demonstrated that tracking the "amplified" diffraction pattern was much more precise to determine the movement of the object within the trap than analyzing the minute motion of the object itself. Displacement of the object could then be translated into the force being applied by the tweezers. Also, using an algorithm developed in the lab, we were able to follow the movement of the scattering pattern at a temporal resolution close to video rate. We have used this system to investigate the binding force associated with cell-cell interactions and molecular interactions. In these studies, a cell was carefully positioned to make contact with another cell or a microparticle coated with proteins of interest by optical tweezers in a well-controlled manner. During these events, we noted a progressive increase of cell adhesion at the immediate early period (i.e., a few minutes after initial contact) of cell-cell interactions. Also, binding of a disintegrin, rhodostomin, and its mutant to the counterpart integrin on the cell surface could be assessed with great convenience and accuracy. Our results demonstrated that addition of the forward scatter analysis module to conventional optical tweezers provides an effective and convenient way for monitoring biological activities *in situ* and measuring changes of biological forces with precision.

Keywords: forward scattering, optical tweezers, adhesion, integrin, disintegrin

1. INTRODUCTION

Forces are involved in proper functioning of tissues and cells, in the processes ranging from muscle contraction (Huxley et al., 1969), morphogenesis during embryonic development (for review, seeSchwarzbauer, 1997), vesicular transport across the cell, and alignment of chromosomes at metaphase plate and subsequent segregation (for review, see Warner et al.). In all these biological activities, forces must be adjusted to proper levels at the right time and the right subcellular loci. At molecular level, it was also clear that proteins such as molecular motors and polymerases could respond to changes in mechanical forces by altering their enzymatic functions (for review, see Khan et al., 1997). Forces associated with these biological events are typically very small, ranging from pico-Newtons (pN) to tens of pN, posing difficulties for quantification and close monitoring of their dynamic changes over time.

Traditionally, forces associated with cell activities were measured mainly by mechanical methods such as attaching fine needles or compliant probes to the motile component of the cell. Spring constants derived from these experiments were then used to calculate the magnitude of forces involved. However, data obtained from such approaches were sometimes varied and the experimental procedures were often time-consuming and/or invasive. Recent technical advances, primarily on atomic force microscopy (for review, see Lal and John, 1994) and laser tweezers (Ashkin et al, 1986), had made possible measuring biological forces at single-cell or molecular level (for review, see Mehta et al., 1999), in a more convenient and consistent way.

* Correspondence: Email: linch@ym.edu.tw; Telephone: 886-2-2826-7219; Fax: 886-2-2821-2880

In *Optical Sensing, Imaging, and Manipulation for Biological and Biomedical Applications*, Robert R. Alfano, Ping-Pei Ho, Arthur E. T. Chiou, Editors, Proceedings of SPIE Vol. 4082 (2000) • 0277-786X/00/$15.00

Microscopic objects, including biological materials, could be remotely manipulated with tightly focused beams of infrared laser light (Ashkin et al, 1987). After focusing by high numerical aperture (N.A.) objectives, light pressure and optical gradient forces of optical tweezers could be used to hold, and therefore move sub-micrometer sized objects, even in the interior of the cells (Ashkin et al, 1990). Using such conventional "single-beam gradient radiation pressure laser traps", we were able to initiate interactions between living cells with accuracy and measure non-invasively an intracellular kinetic activity, called cortical F-actin flow, at a local lamella region in real time (Lin and Forscher, 1995). In addition to micromanipulation, optical tweezers could also be employed to biological force measurement (for review, see Ghislain et al, 1994). Typically, optical tweezers with a working wavelength in the optical window of biological material (700-1100 nm) could exert pN forces. The object trapped in optical tweezers might be viewed as being held in three-dimensional space by elastic springs. By calibrating the displacement with a known force applied to the trapped object, one could obtain the spring constants, and then derive the actual force being applied from these constants in the experiments. However, the range of motion within the trap was usually little (at sub-micron range), making displacement analysis and quantification of the trapped object a very difficult task.

Recent progress in video and digital image processing had made possible measurement of nanometer displacement under a microscope (Gelles et al., 1988; for reviews, see Khan and Sheetz, 1997 and Mehta et al., 1999). By amplifying the contrast of light microscopic images, Sheetz and his colleagues successfully observed in real time the diffraction images of cell structures 10 times smaller than the Raleigh resolution limit of 0.2 μm (Schnapp et al., 1988). In this paper, we have applied the forward-scattered light and used the diffraction images to extract information about motion of the object trapped in the tweezers at sub-nanometer level. This technique enabled us to characterize the immediate early events of cell-cell and molecular interactions with better precision in real time. The integration of a convenient force measurement module to optical tweezers holds great promise to extend the use of the tool, not only for noninvasive micromanipulation but also for mechanical assessment in cell biological studies.

2. EXPERIMENTAL CONFIGURATION

2.1. Optical tweezers

The experimental configuration is shown in Fig. 1. Essentially, a research-grade inverted light microscope was equipped with a single-beam gradient force optical trap (optical tweezers) and a force measurement module based on forward scatter analysis (FORSA). A 100mW CW single-mode diode laser at 830±10nm was used as the trapping beam. The laser beam was collimated and circularized with a collimating lens and a pair of anamorphic prisms, and further expanded by a pair of lens to fill the back aperture of the objective. The lens L1 was mounted on a 3-dimension translation stage for lateral and axial position control of the trap in the specimen plane. The trapping beam was then directed to the objective via a dichroic mirror that reflected near infrared but passed UV/visible light. With careful choice of focal lengths of L1 and L2, lateral translation of L1 was equivalent to angular rotation of the laser beam at the back aperture of the objective, thus preventing power decrease when moving the trap. For trapping polystyrene beads ranging from 1 to 10 micrometer and cells, oil-immersion 100X (NA = 1.25) and 40X (NA = 1.0) objectives, respectively, were employed to bring the laser beam to a diffraction limited focus and produce gradient of light intensity serving as a stable 3-D trap.

For high-resolution position measurement of the bead, a beam from a 15mW Helium-Neon (He-Ne) laser was coupled to the light path of the tweezers serving as the probe. The probing beam was focused by the objective and directed to the same position but on a lower plane of the trapping area. A condenser of NA = 0.7 that originally functioned on the microscope to condense incoherent illumination collected the scattered light transmitted through the sample. When a microsphere was trapped, it acted as a microlens to refract the probing light and produced a high contrast light spot. This pattern was subsequently monitored by a charge-coupled device (CCD) after blocking the trapping beam through an IR filter. The signals were captured and digitized in video rate by an image capture card and analyzed by the program discussed later to find the center of the diffraction spot. We used an advanced fast tracking algorithm that was able to operate during frame capturing, so frame-by-frame analysis could be done on line (i.e., at video rate) with high accuracy.

The microscope system included a fully functional inverted microscope capable of bright field, phase contrast, differential interference contrast (DIC), and fluorescence imaging. Bright field and DIC images were detected by a CCD camera and fluorescence images by a silicon intensified target (SIT) camera. Data was recorded in videotapes or as digital files in the computer.

2.2. Tracking diffraction patterns in real time and force calibration

To measure the stiffness of the optical tweezers, a viscous force was generated by oscillatory motion of the specimen by a DC motor-driven stage at constant velocity. The tracking program tracked the diffraction pattern that reflected the bead position in the trap. Moving beads attached to a coverslip then determined the relationship between the diffraction pattern and bead position.

2.3. Cell Culture

A human embryo kidney cell line HEK-293T and a Chinese hamster ovary (CHO) cell line expressing integrin$\alpha_{IIb}\beta_3$, a gift from Dr. Yoshikazu Takada of the Scripps Research Institute, were used for cell-cell and rhodostomin-integrin interactions, respectively. Cells were grown in Dulbecco's modified Eagle medium (DMEM) supplemented with 10% fetal bovine serum, 0.1 mM non-essential amino acids, 2 mM L-glutamine, and 50 μM gentamycin. HEK-293T and CHO cells were incubated in 8% and 5% CO_2, respectively, at 37 °C. Cells were removed from tissue culture dishes by brief treatment with trypsin-EDTA, and plated onto glass coverslips coated with 0.2mg/ml 70kD poly-L-lysine for 1 hr at 37 °C.

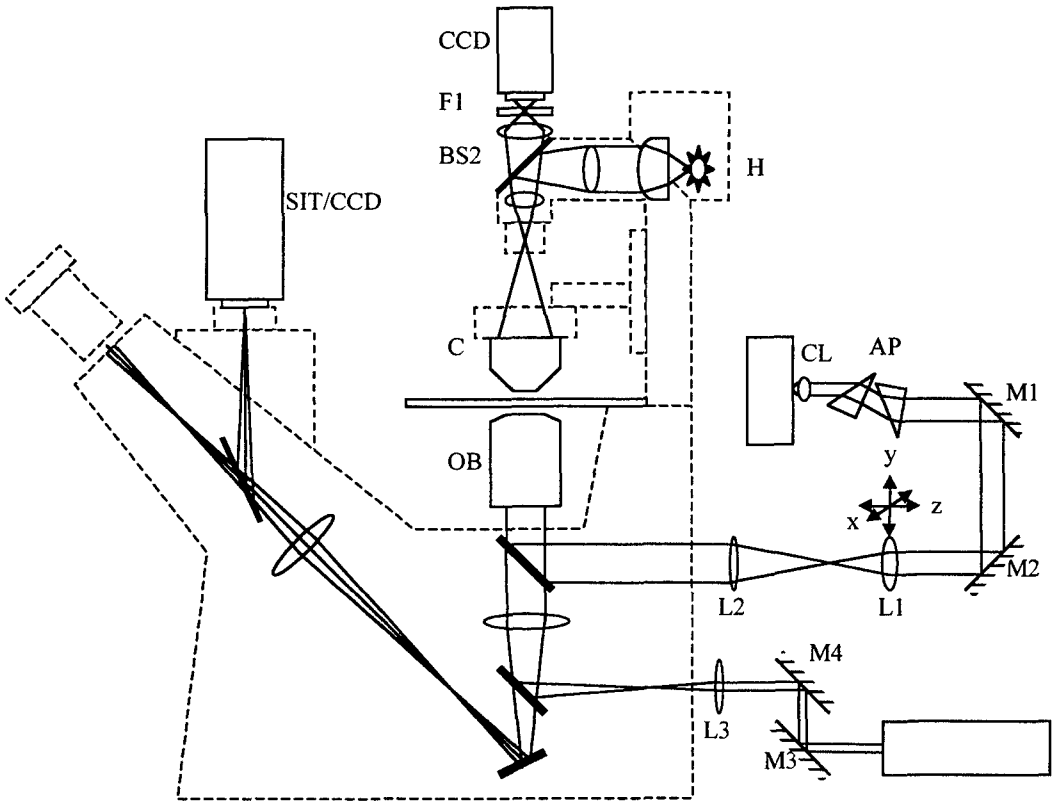

Fig. 1 A schematic illustration of the experimental configuration. The set-up consists of optical tweezers and a force measurement module incorporated into an inverted microscope. A diode laser and a Helium-Neon laser serve as a trapping and a probing beam, respectively. Optics include collimating lens CL and anamorphic prisms AP for collimating and circularizing the trapping beam; mirrors M1, M2, M3, and M4 for beam steering; lenses L1, L2, L3, and L4 for beam expansion and movement. A short-pass dichroic mirror DM1 and a beam splitter BS1 direct the beam to the objective OB and transmit the incoherent illumination to the imaging system. For collection and detection of the scattered light from the probing beam, the condenser C of the microscope is used for light collecting, followed by an IR filter F1 to block the trapping beam. The incoherent illumination for bright field and DIC imaging of the sample includes a halogen lamp H steered by a beam splitter BS2 and condensed by the condenser C, providing Kohler illumination in the specimen field. The fluorescence light path from the epi-fluorescence port is not shown for clarification.

2.4. GST-Rhodostomin Constructs and Protein Purification

The various rhodostomin constructs were kind gifts from Dr. S.J. Lo, Institute of Microbiology & Immunology, National Yang-Ming University, Taipei, Taiwan. Rhodostomin expression plasmids (pGST-RHO(RGD) and pGST-RHO(RGE)) were generated as previously described (Chang et al., 1999). Mutations were made by insertion alanine to amino acid position 48, 52 or 53 (Fig. 5). Synthesis of the GST-fusion proteins was induced in *Escherchia coli* JM109 by adding 0.1M isopropyl-1-thio-β-D-galactopyranoside (IPTG) to the culture medium. Protein in the bacterial lysate was purified by binding to glutathione sepharose 4B and eluted with 10mM reduced glutathione in 50 mM Tris-HCl, pH 8.0.

2.5. Bead Coating

The bead coating utilized physical hydrophobic adsorption. Polystyrene beads were incubated with 0.1 mg/ml of proteins of interest in phosphate buffered saline (PBS) for 1.5 hrs at room temperature and subsequently back coated with 2% bovine serum albumin (BSA) in PBS. The coated beads were kept in 4°C for use in no more than 1 week.

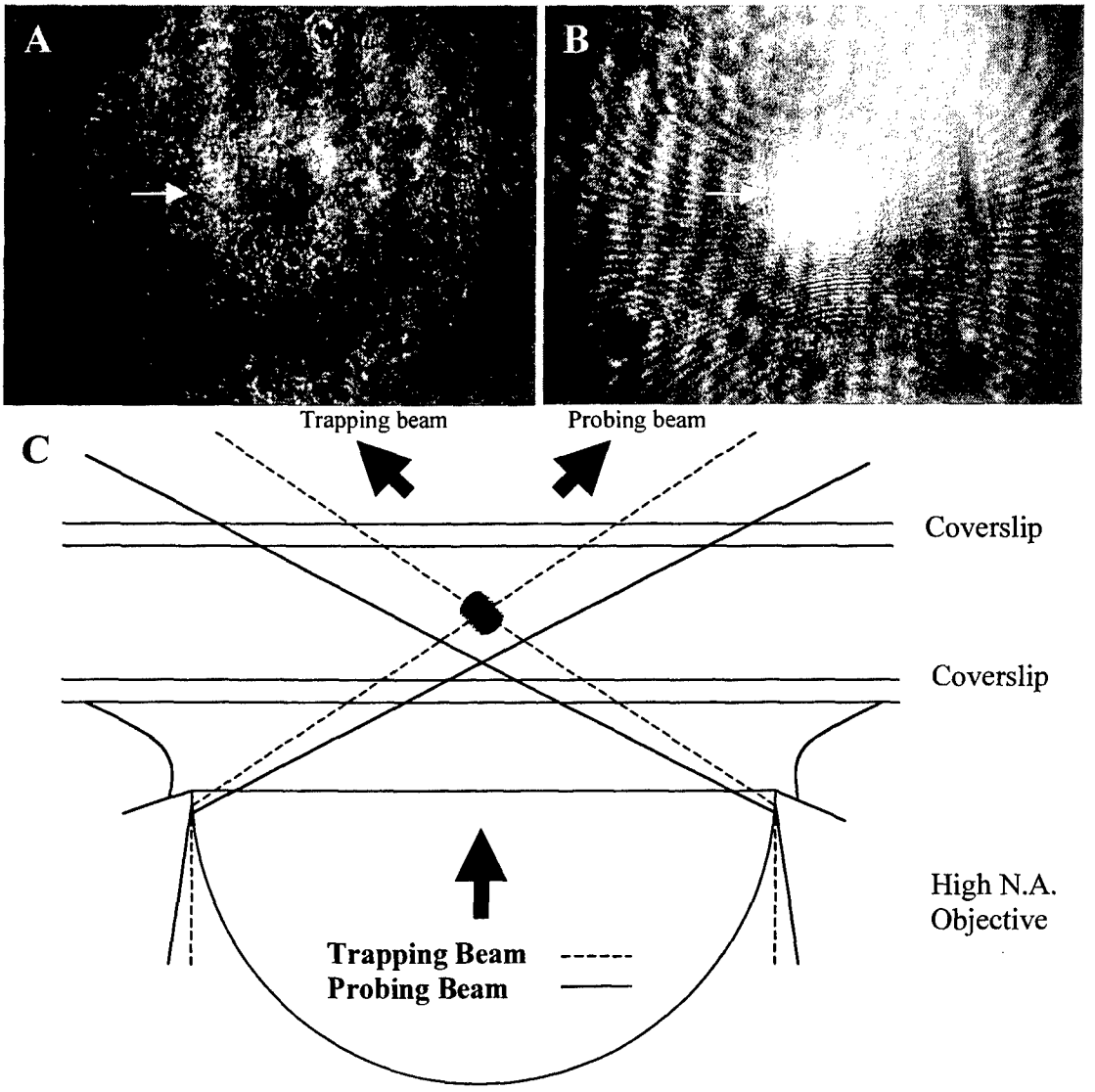

Fig. 2. Improving the image quality of diffraction patterns by addition of a probing Ne-Ne laser. (A) The probing beam was focused at a slightly lower plane than the trapping beam. Diffraction patterns of the trapped bead (*arrows*) generated by either the trapping (B) or probing (C) beam capture from the conjugated aperture planes of the microscope.

3. EXPERIMENTAL RESULTS

3.1. The image quality of scattering patterns was improved by the probing laser

Within the FORSA module (see Materials and Methods and Fig. 1), the probing He-Ne laser (*solid lines*, Fig. 2C) was directed into the light path of the optical tweezers (*dashed lines*, Fig. 2C). The probing beam was focused at a slightly lower plane than the trapping beam and generated a highly contrasted circular scattering pattern of the trapped bead (*arrow*, Fig. 2B) at the conjugated aperture plane of the microscope. Note the trapping beam also formed a ring-shaped scattering pattern (*arrow*, Fig. 2A), but the contrast was very low. In other words, the integrated probing beam dramatically improved the image quality of the scattering pattern and made possible precise tracking of the object movement within the tweezers (see below).

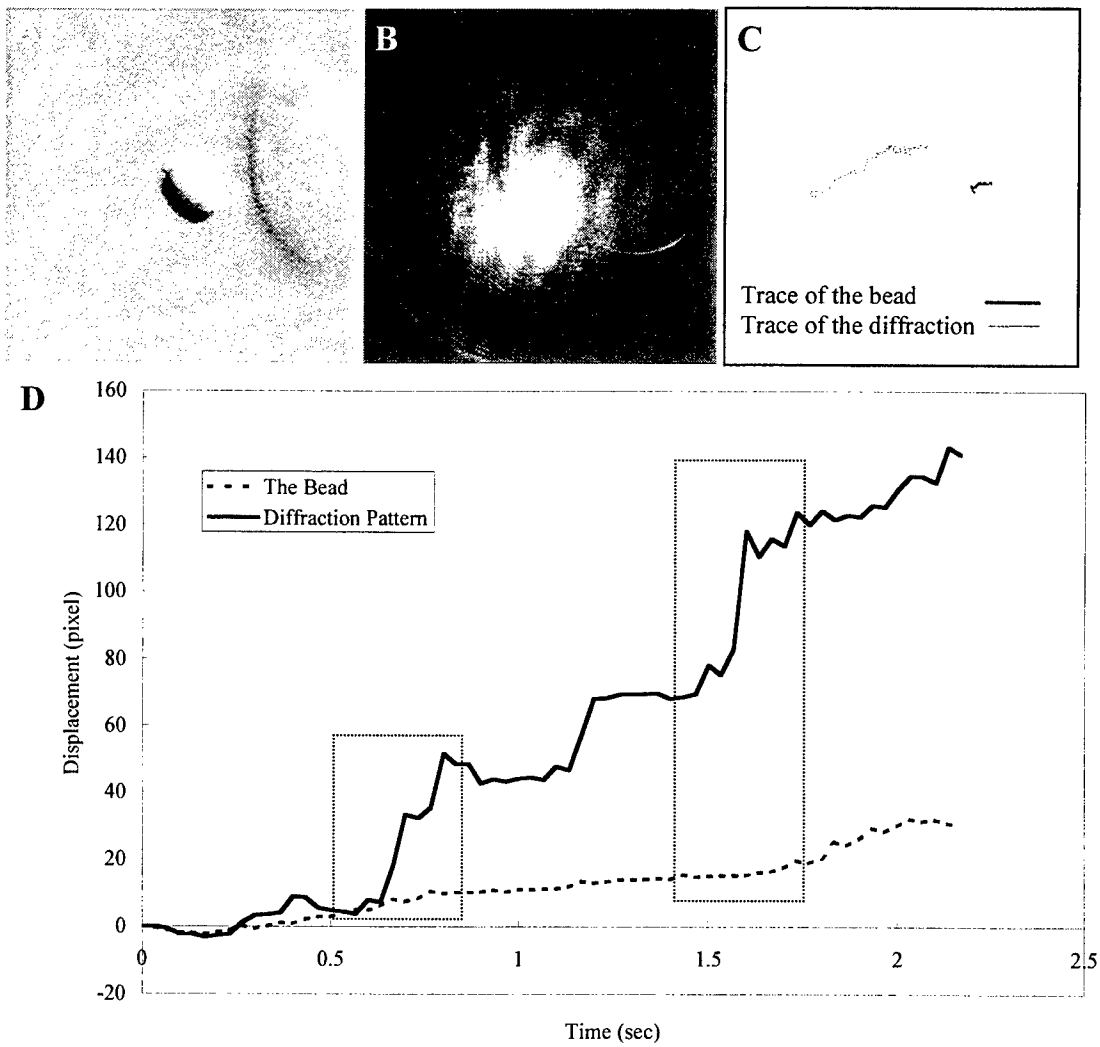

Fig. 3. The displacement of the trapped bead was amplified, and therefore could be better quantified, by following the movement of the diffraction spots. A 7.75μm bead coated with poly-L-lysine was put in contact with a NIH-3T3 cell for 30 sec. The cell was then pulled away from the bead trapped in the tweezers by moving the DC motor-driven microscope stage rightward. The bead (A) and its diffraction pattern (B) generated by the probing beam were simultaneously recorded by two CCD cameras; and their displacement traces (*black line*: bead; *gray line*: diffraction spot) were recorded in real time (C). (D) Detailed analysis of the displacement over time revealed two phases of impulsive advance (*arrows and arrowheads*) that were readily resolved by following the diffraction pattern (*gray trace*), but were hardly visible by monitoring the bead movement (*black trace*).

3.2. Tracing the trapped object with better accuracy and in real time

We then analyzed both the spatial and temporal resolution of the FORSA module. As shown in Fig. 3A, a 7.75 μm polystyrene bead coated with poly-L-lysine made contact with a NIH-3T3 cell for 30 sec and was then pulled away from the cell by moving the DC motor-driven stage rightward at a constant velocity of ~1 micron/sec. There was a membrane tether (not shown at this focal plane) linking the bead and the cell surface as previously described (Dai and Sheetz, 1995; for review, see Sheetz and Dai, 1997). The DIC image of the bead (Fig 3A) and the diffraction pattern at the aperture plane (Fig. 3B) were separately monitored by two different CCD cameras simultaneously, and digitized and analyzed using a program developed in the lab (see Materials and Methods). Note this program enabled us to trace the displacement of the bead and the diffraction spot at a temporal resolution close to video rate (30 frame per second).

As shown in Fig. 3C, the motion of the bead within the tweezers (*black trace*) was greatly amplified by forward scatter analysis (*gray trace*). The displacements of both the bead and the diffraction spot were plotted as a function of time (Fig. 3D). Note detailed analysis of the diffraction trace revealed two obvious impulsive movements which could hardly be identified by following the bead motion (*dashed rectangles*). These two steps of abrupt advance might actually reflect the discontinuous stage motion driven by the DC-motor.

Using fluid flow assay, we estimated that the maximal force our experimental configuration could exert was ~12pN on a 7.75-μm polystyrene bead, and the stiffness was ~3.8 pN/μm (data not shown). Since trapping force exerted on the bead was directly proportional to the displacement of the bead in the tweezers, the FORSA module that gave a more sensitive measure of bead motion should provide a more accurate way for biological force measurement.

3.3. Applications in cell-cell interactions

We then employed optical tweezers to monitor the adhesion force during immediate early period (within just a few minutes) of cell-cell interactions. A HEK-293T cell was manipulated to make contact with another cell already attached to the

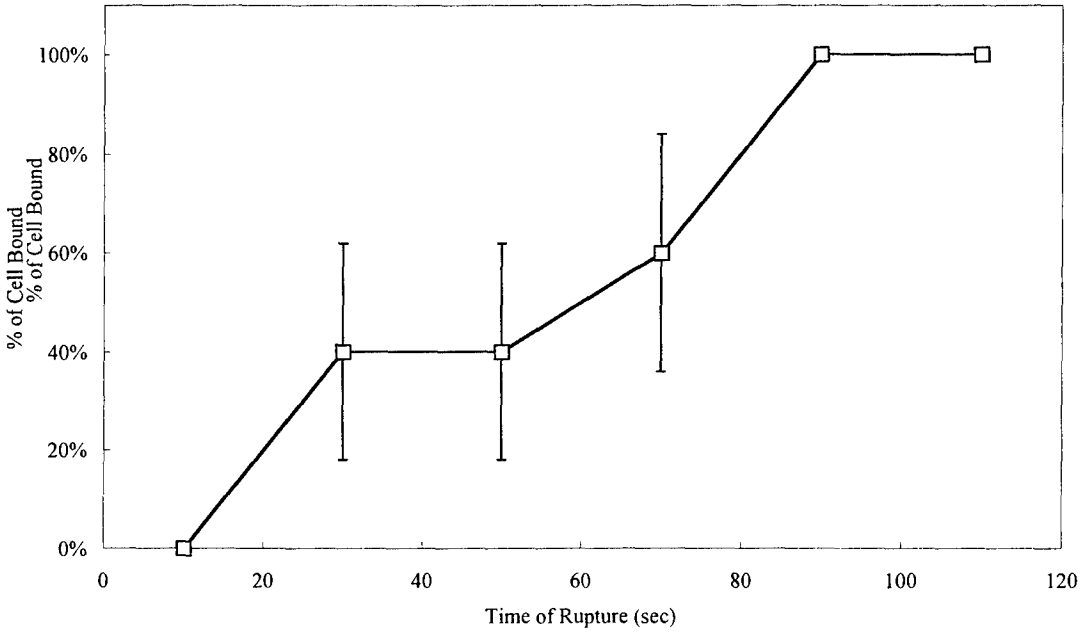

Fig. 4. Adhesion analysis on HEK-293T cells. A HEK-293T cell in the medium was put in contact with another cell tightly attached to the substrate for a period of time (time of rupture) before being pulled apart by optical tweezers exerting approximately 10 pN force. At least 25 pairs of interacting cells were tested in each condition. From this, the percentage of cell pairs that resisted the separation procedure was calculated. Mean ± SE were shown.

substrate. The interacting cells were held for various periods of time (termed rupture of time, Fig. 4), and then pulled apart by a maximal force exerted by the optical tweezers (approximately 12 pN). At least 25 pairs of cells were tested in each condition. The percentages of cell pairs that resisted the pulling and remained adhered were plotted as a function of rupture of time (from 10 to 110 sec). As shown in Fig. 4, we found a progressive increase of cell adhesion, about 50% of the cell pairs were tightly adhered one minute after the contact and in two minutes none of the cell pairs could be pulled apart by ~12 pN force.

3.4. Applications in integrin-disintegrin interactions

In another set of experiments, we have used optical tweezers to analyze the binding between disintegrin and integrin proteins. To facilitate the force measurement, we placed a kind of disintegrins, the snake venom rhodostomin, and its mutants each containing single amino acid insertion at the peptide position of 48th, 52nd or 53rd amino acid, on 7.75 μm polystyrene beads. These uni-sized beads provided a uniform pulling force for assessing the binding between integrin and disintegrin proteins. Beads coated with different rhodostomin constructs were held, and then interacted with CHO cells expressing the receptor integrin $\alpha_{IIb}\beta_3$ for different periods of time (rupture of time) before being pulled away with maximal trapping force. At least 20 beads were tested in each condition. As shown in Fig. 5, the percentage of beads that resisted pulling, i.e., remained bound to the cells, were plotted as a function of rupture of time (from 0 to 90 sec). Note beads coated with wild-type rhodostomin, containing the RGD sequence at position 49-51 (RGD), exerted the strongest binding to the

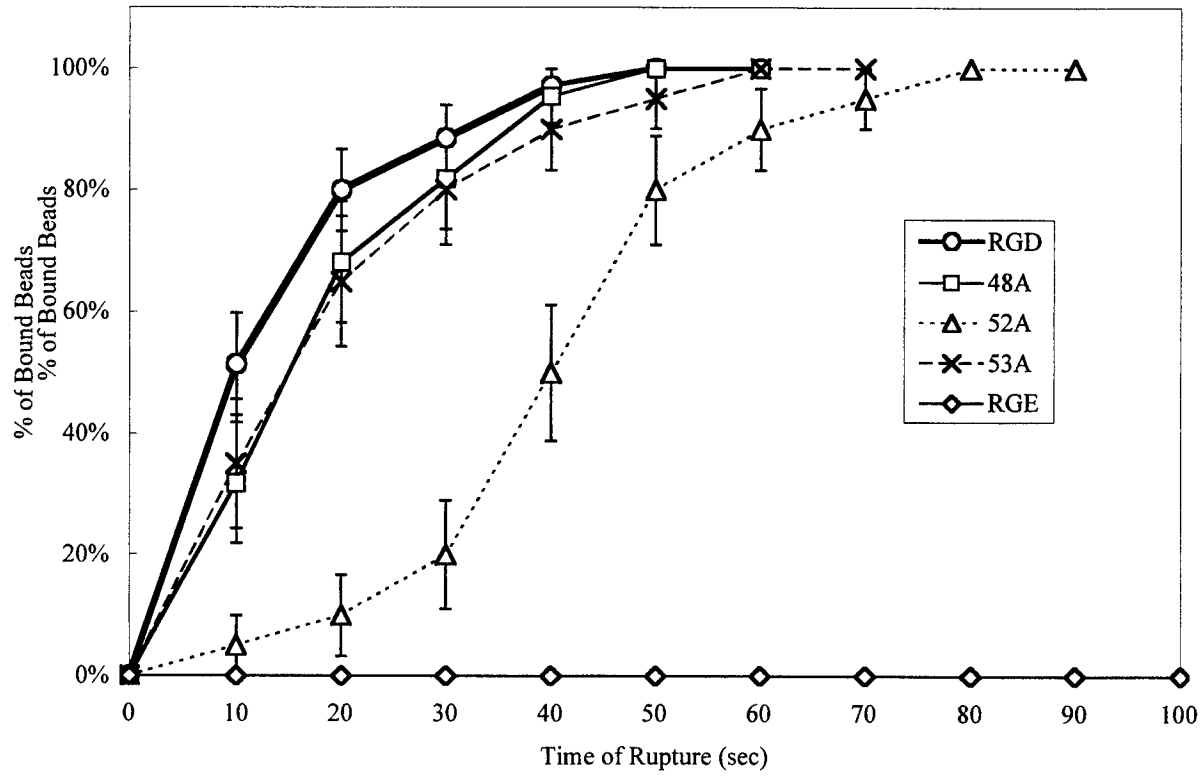

Fig. 5 Interactions between beads coated with different recombinant rhodostomin proteins and CHO cells steadily expressing integrin$\alpha_{IIb}\beta_3$. Beads were positioned and held to the cell surface for different periods of time (time of rupture) before being pulled away with optical tweezers exerting ~12 pN force. The proportion of beads that remained attached to the cell were then calculated (Mean ± SE, n = 20-30 beads). Note beads coated with wild-type rhodostomin, containing the RGD sequence at position 49-51, exerted the strongest binding to the cell. Within 10 sec after initial contact, more than 50% of the beads resisted the separation procedure. An insertion of alanine at the position of 48th or 53rd amino acid (48A and 53A, respectively) slightly decreases the binding affinity whereas addition at the 52nd amino acid drastically decreased the binding and hence increased the time of rupture. Replacing the RGD sequence motif of the rhodostomin with the RGE sequence essentially abolishes the binding between rhodostomin and integrin; no significant binding was found even after 5 min of interactions.

cell. Within 10 sec after initial contact, more than 50% of the beads became tightly associated with the cell. Insertions of alanine at the 48th or 53rd amino acid (48A and 53A, respectively) only slightly affected the binding affinity whereas addition at the 52nd amino acid of rhodostomin (52A) significantly reduced the binding of the mutated rhodostomin to integrin $\alpha_{IIb}\beta_3$. These findings were in good agreement with biochemical results and/or cell-attachment experiments performed on different rhodostomin-coated substrates (data not shown, but see Chang et al., 1999). Also consistent with previous investigations (Chang et al., 1997, 1998, 1999), replacing RGD sequence motif of rhodostomin with RGE (RGE) essentially abolished the binding between the integrin and disintegrin protein.

4. SUMMARY AND CONCLUSION

In the present study, we have constructed a functional module that could be easily integrated into conventional optical tweezers (Fig. 1). Since the entire design was based on forward scattered light analysis, this system was dubbed the FORSA module. Several improvements were achieved by the addition of an auxiliary off-focus probing beam to the system. These include: (1) The contrast of diffraction patterns from the trapped object was greatly enhanced compared to the contrast generated by the trapping beam (Fig. 2). The better image quality obtained significantly increased the accuracy for displacement analysis. (2) The motion of the object within the tweezers, indicative of the force being applied, could be effectively amplified by analyzing the diffraction pattern (Fig. 3) which combined with (3) the fast tracking algorithm that monitored the central maximum of the scattered light at a temporal resolution close to video rate, made possible a new way of measuring biological forces with improved accuracy and in real time.

Although forward scatter analysis was successfully applied to optical tweezers for trapping and force measurement, the relationship between the extent of "off-focusing" of the probing beam and the size of bead being trapped have not yet been determined. It was clear from our experiences that the focusing position of the probing beam significantly influenced the quality of diffraction patterns. Also important is the numerical aperture (NA) of the objectives used for trapping and probing since the unscattered background is proportional to NA. Using beads of smaller sizes, for example requires a decrease in the NA of the objectives to optimize the contrast because increased unscattered light are produced by smaller beads.

The addition of a probing beam provided not only better contrast but also extra flexibility for incorporating different illumination methodologies. For example, we have applied an annular aperture to this system; the resulting donut-shaped probing beam appeared to greatly decrease the background of unscattered light and, as a result, enhanced signal to noise ratio (S/N ratio) of the system (Tsai et al., manuscript in preparation). Other kinds of modulation of the probing laser were also under investigation aiming to improve the S/N ratio and the sensitivity/accuracy for displacement analysis.

Using the FORSA algorithm developed in our lab, we were able to follow the movement of the diffraction spot "on-line" or close to video rate (~33 ms). Current temporal resolution was actually limited by our detection system, the CCD camera and NTSC analog format, which could be further improved to up to sub-nanosecond level by using a quadral photodiode for detection.

Two experimental biological systems were tested for optical tweezers applications. In cell adhesion experiments, we were able to monitor and resolve the progressive adhesion between cells held by optical tweezers (Fig. 4). This tool provided us with a unique way to make measurements on individually selected cells and within a very precise window of time (for example, the first few seconds after cell-cell or molecular contact), which is very difficult to analyze using other methodologies. Similar advantages could be extended to experiments addressing molecular interactions (Fig. 5). Different binding affinity between molecules containing single amino acid change could be readily identified and quantified by our system. More importantly, using micron-sized beads as probes also makes possible the measurement of receptor density on the cell surface during various physiological and pathological conditions (Tsai, Yi et al., manuscript in preparation). We believe that the new tool described in this report would help tremendously in on-line monitoring and/or analysis of biological activities *in situ*, such as initial events of cell-cell and ligand-receptor interactions, which might occur within seconds and are difficult to study using traditional biochemical assays. The FORSA system represents an intuitive and easy-to-install solution for trapping as well as force measurement with higher accuracy and convenience than direct visualization of the trapped objects themselves.

ACKNOWLEDGEMENTS

The authors gratefully acknowledge Dr. Pei-Hsi Tsao of National Taiwan University and Dr. Szecheng J. Lo of NationalYang-Ming University for the inspiration and valuable comments, and Dr. Yoshikazu Takada of the Scripps Research Institute for providing the cell lines. Also thanks to Chih-Pei Chang and Yong-Shyang Yi for providing the wonderful rhodostomin system. Special thanks to Weber Chen for his superior technical assistance. The works were supported by grants from Frontier Medical Genomic Program, and Program for Promoting Academic Excellency, and National Science Council, NSC89-2318-B-010-002-M51 awarded to CHL.

REFERENCES

1. Ashkin, A., Dziedzic, J. M., Bjorkhlm, J. E., and Chu, S., "Observation of a sigle-beam gradient force optical trap for dielectric particles," *Optics Lett.* **11**, pp. 288-290, 1986.
2. Ashkin, A., Dziedzic, J. M. and Yamane, T., "Optical trapping and manipulation of single cells using infrared laser beams" *Nature* **330**, pp. 769-771, 1987.
3. Ashkin, A., Schutze, K., Dziedzic, J. M., Euteneuer, U., and Schliwa M., "Force generation of organelle transport measured in vivo by an infared laser trap," *Nature* **348**, pp. 346-348, 1990.
4. Chang H. H., Tsai W. J., and Lo S. J., "Glutathione S-transferase-rhodostomin fusion protein inhibits platelet aggregation and induces platelet shape change," *Toxicon.* **35(2)**, pp. 195-204, 1997.
5. Chang H. H. and Lo S. J., "Full-spreading platelets induced by the recombinant rhodostomin are via binding to integrins and correlated with FAK phosphorylation," *Toxicon.* **36(8)**, pp. 1087-99, 1998.
6. Chang H. H., Lin C. H., and Lo S. J., "Recombinant rhodostomin substrates induce transformation and active calcium oscillation in human platelets," *Experimental Cell Research* **250(2)**, pp. 387-400, 1999.
7. Dai, J. and Sheetz, M. P., "Mechanical properties of neuronal growth cone membranes studied by tether formation with laser optical tweezers," *Biophys. J.* **68**, pp. 988-996, 1995.
8. Dai, J. and Sheetz, M. P., "Axon membrane flows from the growth cone to the cell body," *Cell* **83**, pp. 593-901, 1995.
9. Gelles J., Schnapp B. J., and Sheetz, M.P., "Tracking kinesin-driven movements with nanometre-scale precision," *Nature*. **331(6155)**, pp. 450-453, 1988.
10. Ghismain, L. P., Switz, N. A., and Webb, W. W., "Measurement of small fores using an optical trap," *Rev. Sci. Instr.* **65**, pp. 2762-2768, 1994.
11. Huxley, H. E., "The mechanism of muscular contraction," *Science* **164**, pp. 1356-1366, 1969.
12. Khan, S., and Sheetz, M. P., "Force effects on biochemical kinetics," *Annual Review of Biochemistry* **66**, pp. 785-805, 1997.
13. Lal, R. and John. S., "A. Biological applications of atomic force microscopy," *Am. J. Physiol.* **266** (*Cell Physiol.* **35**), pp. C1-1-221, 1994.
14. Lin, C. H. and Forscher, P., "Growth cone advance is inversely proportional to retograde F-actin flow," *Neuron* **14**, pp. 763-771, 1995.
15. Mehta, A. D., Rief, M., Spudich, J. A., Smith, D. A., and Simmons, R. M., "Single-molecule biomechanics with optical methods," *Science*. **283(5408)**, pp. 1689-95, 1999.
16. Schnapp, B. J., Gelles, J., Sheetz, M. P., "Nanometer-scale measurements using video light microscopy," *Cell Motility & the Cytoskeleton.* **10(1-2)**, pp. 47-53, 1988.
17. Schwarzbauer, J. E., "Cell migration: may the force be with you," *Current Biology*. **7(5)**, pp. R292-4, 1997.
18. Sheetz, M. P. and Dai, J, "Modulation of membrane dynamics and cell motility by membrane tension," *Trends Cell Biol.* **6**, pp. 85-89, 1996.
19. Warner, F. D. and McIntosh, J. R. (eds) in *Cell Movement* Vol. 2 Liss, New York, 1989.
20. Yin, H., Wang, M. D., Svoboda, K., Landick, R., Block, S. M., Gelles, J., "Transcription against an applied force," *Science* **270**, pp. 1653-1657.